Acta Crystallographica Section A
Foundations of Crystallography
ISSN 0108-7673

Received 3 May 2000
Accepted 24 July 2000

On possible extensions of X-ray crystallography through diffraction-pattern oversampling

J. Miao*† and D. Sayre‡

Department of Physics and Astronomy, State University of New York, Stony Brook, NY 11794, USA. Correspondence e-mail: miao@ssrl.slac.stanford.edu

It is known that sampling the diffraction pattern of a finite specimen, at a spacing somewhat finer than the Nyquist spacing (the inverse of the size of the diffracting specimen), corresponds to generating a no-density region surrounding the electron density of the specimen. This no-density region can then be used to retrieve the phase information. In earlier papers [Miao, Sayre & Chapman (1998). *J. Opt. Soc. Am.* A**15**, 1662–1669; Sayre, Chapman & Miao (1998). *Acta Cryst.* A**54**, 232–239], it was demonstrated, in the case of non-crystalline specimens, that this no-density region could be used to retrieve the phase information; here the same is performed for crystalline and near-crystalline specimens. By employment of an iterative algorithm, the phase information could be recovered from computer-generated oversampled diffraction patterns of small specimens that are (*a*) perfect or imperfect crystals, or (*b*) have a repeated motif without orientational regularity, or (*c*) are an unrepeated motif, such as an amorphous glass, a single molecule or a single biological cell. Cases (*a*) and (*b*) represent an extension over work recently published [Miao, Charalambous, Kirz & Sayre (1999). *Nature (London)*, **400**, 342–344]. Our algorithm requires an approximate envelope for the specimen. It does not require any structural knowledge concerning the specimen and does not require data to atomic resolution (although it can use such data if present). After a few hundred to a few thousand iterations, the correct phase set and image are recovered. The oversampling technique thus greatly extends the specimen range of X-ray crystallography but it imposes a high radiation dose on the specimens compared with the situation in crystallography, in which it is usual for the pattern to be sampled at the (much less fine) Bragg spacing (the inverse of the size of the unit cell). In cases where the specimen is a crystal, there are also possibilities for oversampling relative to Bragg (instead of Nyquist) sampling, thus providing a lesser degree of oversampling and the possibility of lower dosage. Damage of the specimen in consequence of the dose will in many cases seriously affect the quality and resolution of the imaging, but in at least one case [the biological cell in (*c*) above] the imaging obtainable with the aid of a cryogenic protective technique should surpass any other present method of whole-cell imaging. In addition, with the possible appearance in the future of free electron lasers ($>10^{12}$ photons and <200 fs per pulse), it is possible to circumvent the radiation-damage problem by recording diffraction patterns before damage manifests itself.

© 2000 International Union of Crystallography
Printed in Great Britain – all rights reserved

1. Introduction

When an object is illuminated by a plane wave, the scattered wave in the far field forms, within the Born approximation, the Fourier transform of the object. While the magnitude of the Fourier transform pattern can be recorded by a detector, the phase of the pattern is lost. To reconstruct the electron density of the object, however, the phase information must be known. This constitutes the well known phase problem. The phase problem is somewhat different for non-crystalline specimens and crystals. When a specimen is non-crystalline, the diffraction pattern is faint and continuous. This continuous pattern can therefore be sampled on a finer spatial scale than the Nyquist frequency, where the Nyquist frequency (f_N) is defined as $f_N = 1/s$ for a specimen with size s. (It turns out that

† Present address: SSRL, PO Box 20450 MS 69, Stanford, CA 94309-0210, USA.
‡ Mailing address: 427 Monroe Street, Bridgewater, NJ 08807, USA.

the Nyquist frequency is the minimum sampling frequency for the Fourier transform to invert to the correct image when the magnitude and phase are known.) Partially following the ideas from Boyes-Watson *et al.* (1947), Sayre (1952) and Bruck & Sodin (1979), Bates (1982) suggested that oversampling the diffraction pattern could lead to the phase information. Based on the argument that the autocorrelation function of any sort of image is twice the size of the image itself in each dimension, Bates concluded that the phase information could be retrieved by oversampling the magnitude of a Fourier transform at least twice as finely as Nyquist frequency (meaning 4× for two dimensions and 8× for three dimensions). Millane (1996) showed that Bates's sampling criterion can be reduced somewhat in the three-dimensional or more case. The suggestion that the oversampling technique could be applied in X-ray diffraction studies was made by Sayre (1991). Recently, we have made progress in understanding the applicability of the oversampling technique to the phase problem. We proposed a theory to explain the oversampling technique and showed that, given the magnitude of the Fourier transform sampled at the Nyquist frequency, the phase problem is underdetermined by a factor of 2 for one-dimensional, two-dimensional and three-dimensional objects (Miao *et al.*, 1997, 1998) (instead of factors of 4 and 8 for two-dimensional and three-dimensional objects).

Historically, the phase problem in crystallography has been different, in that normally the Bragg peaks but not the intensity between the Bragg peaks have been recorded. Constructive interference among the large number of identical unit cells generates strong Bragg peaks, which facilitates the data collection and makes the radiation-damage problem to the specimen much less severe than for the non-crystalline specimens. Because of the extreme importance of structure determination by X-ray crystallography, the crystallographic phase problem has been intensively studied and a considerable number of phasing techniques have been developed to retrieve the phase from the Bragg peaks alone (Woolfson, 1987; Millane, 1990). The situation explored in the present paper, however, is what occurs if intensities can also be measured between the Bragg points.

In recent papers (Miao *et al.*, 1999*a*,*b*), we have shown that, by oversampling the diffraction pattern, non-crystals can be imaged by crystallography methods. In this paper, we now extend this remark to the specimens that are (*a*) perfect or imperfect crystals, or (*b*) have a repeated motif without orientational regularity, as well as the previously discussed case of an unrepeated motif, such as an amorphous glass, a single molecule or a single biological cell. When a crystalline specimen is small, both the Bragg peaks and the intensity between the Bragg peaks (an oversampled pattern) can be measured. When a specimen is non-crystalline, the Bragg peaks disappear and the diffraction intensity continuously distributes in reciprocal space that can be oversampled. In either case, the oversampled diffraction pattern can then be used to recover the phase information. In §2, we will discuss the oversampling theorem. In §3, we will show some examples of phase retrieval from both noise-free and noisy oversampled diffraction patterns. Since the whole diffraction pattern, and not just the strong Bragg peaks, is employed for phase retrieval, the oversampling technique faces a major hurdle – the radiation-damage problem, which we will discuss in §4.

2. The oversampling technique

The oversampling technique can be explained by considering a non-crystalline specimen. Fig. 1(*b*) shows a finite specimen and Fig. 1(*a*) its Fourier transform or diffraction pattern. If the latter is sampled at the Nyquist sampling frequency, producing an $N \times N$ array, and the array is re-inverted by fast Fourier transform (FFT) (here we use the term FFT instead of DFT at a reviewer's request to eliminate confusion between discrete Fourier transform and difference Fourier transform), the result is an $N \times N$ array in which the specimen essentially fills the array. However, if the sampling is at twice the Nyquist frequency, the reinversion produces a larger array in which the specimen image is as before, but is now bordered by a no-density region (see Appendix *A*). Obviously, the higher the oversampling degree, the bigger the no-density region. To characterize the degree of oversampling, we define the oversampling ratio (σ) in real space as

$$\sigma = \frac{\text{electron density region} + \text{no-density region}}{\text{electron density region}}. \quad (1)$$

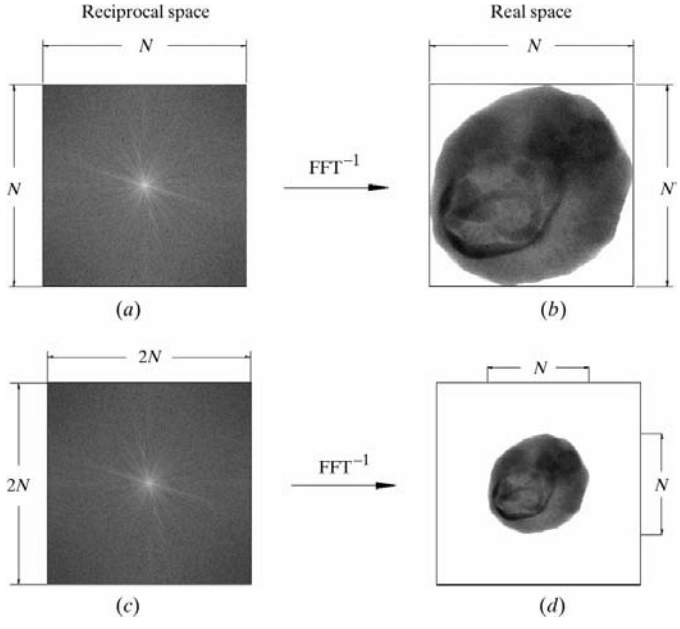

Figure 1
Comparison of Nyquist sampling and finer-than-Nyquist sampling. (*a*) The Fourier transform (diffraction pattern) of a specimen (*b*). The pattern is sampled at the Nyquist frequency and the resulting array will be submitted to inverse fast Fourier transform processing (FFT^{-1}). (*b*) Result of the processing. The specimen essentially fills the result array. (*c*) The pattern sampled at twice the Nyquist frequency. [The array sizes in (*c*) and (*d*) are 4× larger than in (*a*) and (*b*), but for convenience are shown here at the same size.] (*d*) The specimen now is surrounded by an extensive no-density region, which can be used (see Fig. 2 and the discussion in §3) to produce the correct phases and image.

We previously showed that the phase retrieval from an oversampled diffraction pattern is possible only if $\sigma > 2$ (Miao *et al.*, 1998). Emphasis should be made here that (1) represents a no-density region surrounding the whole crystal, which is somewhat different from surrounding the molecule in the unit cell by solvent (see *e.g.* Millane, 1993). Oversampling a diffraction pattern alone cannot lead to a unique phase, however. This is because one cannot distinguish a phase and its conjugate from the diffraction intensity alone, leading to an ambiguity analogous to the twin image problem in holography. To remove this ambiguity, we employ positivity constraints. When the incident X-rays are high-energy photons (hard X-rays) and also away from the absorption edges, the electron density of the specimen is real and positive. When the incident X-rays are low-energy photons (soft X-rays), the electron density is complex. The real part of the complex density represents the effective number of electrons that diffract the X-rays in phase. It is usually positive and only goes negative when the energy of the incident X-rays is near an absorption edge. The imaginary part represents the absorption of the X-rays by the specimen and thus is always positive. These observations were experimentally verified by Henke *et al.* (1993). We thus can apply the positivity constraints on either the real part or the imaginary part to eliminate the conjugate ambiguity. (Our computer modeling seems to show that enforcing the positivity constraints on both parts is not as effective as enforcing them on either the real or the imaginary part.)

The oversampling technique, at least in principle, also solves the phase problems of perfect or imperfect crystals (see the examples of the next section). The method is probably most practical for very small crystals. For large crystals, the added sampling points between the Bragg points will be extremely numerous and faint compared to the Bragg points. This is due to the difference of the two sampling frequencies: the Nyquist frequency (f_N) and the Bragg-peak frequency (f_B). They are related by

$$f_N = f_B M, \tag{2}$$

where M is the number of unit cells in one dimension. Equation (2) shows that the Nyquist frequency is equal to the Bragg-peak frequency for non-crystalline specimens ($M = 1$), but is much higher than the Bragg-peak frequency for large crystals ($M \gg 1$). In the case of a perfect crystal, only the electron density inside a unit cell is to be retrieved. The necessary sampling frequency can therefore be reduced to a value that is only somewhat larger than the Bragg frequency.[1]

3. Computer modeling examples

To apply the oversampling technique to the problem of phase retrieval, we developed an iterative algorithm by modifying the algorithm used in optics, astronomy and imaging (Gerchberg & Saxton, 1972; Fienup, 1982; Millane & Stroud, 1997). The algorithm employs an oversampled diffraction pattern and outputs a correct electron density, and is schematically shown in Fig. 2. Each iteration of the algorithm consists of the following steps.

(I) From the magnitude of an oversampled Fourier transform and a current set of phases (a random phase set for the initial iteration), a Fourier transform $[F_j(\mathbf{k})]$, shown in Fig. 2(*a*), is assembled where subscript j represents the jth iteration.

(II) By applying the inverse FFT to the assembled Fourier transform, we get a density $[\rho'_j(\mathbf{x})]$ shown in Fig. 2(*b*).

(III) We define a boundary to separate the electron density region and the no-density region. Owing to the experimental difficulty of precisely determining the envelope of the specimen, we choose the boundary somewhat bigger than the envelope, *i.e.* a loose support, to allow for uncertainties in determining the envelope. We then enforce constraints in real space. For the density outside the loose support, where the loose support is the small square shown in Fig. 2(*c*), we drive it close to zero based on the following equations:

$$\rho_{j+1}(\mathbf{x}) = \rho_j(\mathbf{x}) - \beta_1 \rho'_j(\mathbf{x}), \quad \mathbf{x} \in S_1 \text{ or } S_2 \tag{3a}$$

or

$$\rho_{j+1}(\mathbf{x}) = \begin{cases} \rho_j(\mathbf{x}) - \beta_2 \rho'_j(\mathbf{x}), & \mathbf{x} \in S_1 \\ \rho_j(\mathbf{x}) - \beta_3 \rho'_j(\mathbf{x}), & \mathbf{x} \in S_2, \end{cases} \tag{3b}$$

where S_1 and S_2 are the regions shown, β_1, β_2 and β_3 are constants that in our reconstructions are set to 0.9, 0.7 and 0.9, respectively. While (3*a*) represents a symmetrical reconstruc-

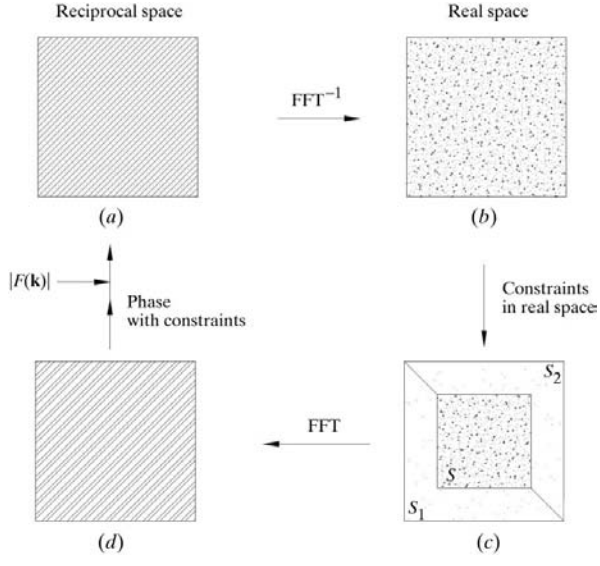

Figure 2
An iterative algorithm for phase retrieval of oversampled diffraction patterns. (*a*) An oversampled Fourier transform combining the magnitude of the Fourier transform and a current phase set. (*b*) An electron density obtained by applying the inverse FFT to (*a*). (*c*) The electron density in regions S_1 and S_2 is driven close to zero and the negative part of the electron density in region S is pushed close to zero, where the little square is a loose support. (*d*) A new oversampled Fourier transform obtained by applying the FFT to (*c*).

[1] This sampling will produce the unit cell surrounded by a no-density region. Again, if the ratio (σ) is bigger than 2, *i.e.* the no-density region is bigger than the electron-density region, the phase information of the unit cell can be retrieved.

tion, (3*b*) is an asymmetrical one and can sometimes speed up the convergence of the reconstruction by quickly eliminating the ambiguity of a phase and its conjugate. We adopt (3*b*) for most of our reconstructions. Inside the finite support, if both the real part and imaginary part of the electron density are positive, we leave the density as it is. Otherwise, the negative part of the electron density is pushed close to zero by the following equation:

$$\rho_{j+1}(\mathbf{x}) = \rho_j(\mathbf{x}) - \beta_4 \rho'_j(\mathbf{x}), \quad \mathbf{x} \in S \text{ and } \rho'_j(\mathbf{x}) < 0, \qquad (4)$$

where S represents the region inside the loose support and β_4 is set to 0.9 in our reconstructions.

(IV) By applying FFT on the new density, we get a new Fourier transform. We adopt the phases from the Fourier transform (also restoring the phase of the central pixel to zero) and thereby obtain a new phase set. It turns out that the constraint of setting the phase of the central pixel to zero can greatly speed up the convergence of our algorithm. (For a complex electron density, the re-setting of the phase of the central pixel to zero may not be applicable.)

The algorithm iterates between reciprocal and real space. In reciprocal space, the magnitude of the Fourier transform is employed in each iteration. In real space, the electron density outside the loose support is gradually pushed close to zero, and the negative part of electron density inside the loose support is driven close to zero. We previously showed that a non-trivial unique phase set exists in an oversampled diffraction pattern provided $\sigma > 2$ and positivity constraints on the electron density (Miao *et al.*, 1998). Usually, after a few hundred to a few thousand iterations, the correct phase set can be retrieved.

By employing the algorithm mentioned above, we have performed a few computer modeling reconstructions of specimens with real and positive electron density. The first example is a two-dimensional small crystal with a 300×300 pixel array shown in Fig. 3(*a*). The crystal consists of 15×15 unit cells and has a size of 75×75 nm. Each unit cell (Fig. 3*b*) has a size of 5×5 nm and 25 randomly distributed 'atoms'. We then border the electron density of the crystal with zero-valued pixels and generate a 512×512 pixel array. By applying a FFT to the array, we calculate the oversampled diffraction pattern of the small crystal. This process is mathematically equivalent to calculating the oversampled diffraction pattern directly from the crystal structure of Fig. 3(*a*) by using Fourier integration instead of FFT (see Appendix *A*). Fig. 3(*c*) shows the oversampled diffraction pattern in linear scale of which we truncate the value of the central pixel in order to display all of the Bragg peaks. Although one cannot see the intensity between Bragg peaks in Fig. 3(*c*), it clearly shows up in Fig. 3(*d*), where the same diffraction pattern is displayed on a logarithmic scale. To reconstruct this diffraction pattern, we define a loose support of a 312×312 pixel (or 78×78 nm) square, which corresponds to $\sigma = 2.7$. By employing the loose support, a random phase set and the positivity constraints on the real part of the electron density, we reconstruct the electron density of the whole small crystal. Figs. 3(*e*), (*f*) and (*g*) show the reconstructions after 0, 50 and 400 iterations, respectively, where the white area represents the no-density region. After 400 iterations, a perfect reconstruction is obtained and the reconstructed unit cell is shown in Fig. 3(*h*). The computing time of 400 iterations is ~10 min on a 450 MHz Pentium II Workstation. Fig. 3(*i*) illustrates the convergence of the reconstruction. The error function used to identify convergence of a solution for an unknown structure is defined as

$$E_j = \left[\sum_{\mathbf{x} \notin s} |\rho'_j(\mathbf{x})|^2 \Big/ \sum_{\mathbf{x} \in s} |\rho'_j(\mathbf{x})|^2 \right]^{1/2}. \qquad (5)$$

We have performed a few more reconstructions of the same diffraction pattern with different initial random phase sets and find that the reconstructions always succeed, but the convergence speed is somewhat different in each case.

To examine the applicability of this approach to experimental data, we have to study the sensitivity of the algorithm to noise. In our computer modeling, we add a random noise defined as

$$\text{Noise} = \text{Signal}/\text{SNR} \times \text{Random} \qquad (6)$$

to the diffraction pattern, where Signal refers to the intensity of the diffraction pattern, SNR is the desired signal-to-noise ratio and the Random function generates an array with its dimension the same as that of the diffraction pattern and each pixel value randomly selected between -0.5 and 0.5. We then add the array of Noise on the diffraction pattern of Fig. 3(*c*) with SNR = 20, 10 and 5, respectively. Our algorithm successfully reconstructs them all. Figs. 3(*j*) and (*k*) show the reconstructed electron density of the whole small crystal and the unit cell with SNR = 10. [For simplicity, we define SNR here as a constant instead of a function of signal. A better noise model would be SNR = $(\text{Signal})^{1/2}$. Future work on this aspect of the method is in progress.]

The next test specimen is the same small crystal but with a few defects inside as Fig. 4(*a*) shows. We then border the 300×300 pixel array specimen with zero-valued pixels and generate a 512×512 pixel array. By applying a FFT to the array, we calculate an oversampled diffraction pattern shown in Fig. 4(*b*). By enforcing the positivity constraints on the real part of the electron density and using the same loose support of a 312×312 pixel square ($\sigma = 2.7$) and a random initial phase set, we reconstruct the electron density from the diffraction intensity. Fig. 4(*c*) shows a perfect reconstruction after 1500 iterations. We then add noise of SNR = 20 on the diffraction pattern. Fig. 4(*d*) shows a good reconstruction after 2500 iterations. We have also performed a few more reconstructions with different initial random phase sets and sometimes get the reconstructed density with the six defects at the centrosymmetrically inverted positions. We believe that this alternate solution is due to the ambiguity of the phase and its conjugate and will further study this phenomenon.

In the next example, we use the same specimen but with each unit cell at random orientation as shown in Fig. 5(*a*). Fig. 5(*b*) illustrates the calculated oversampled diffraction pattern of the specimen. Owing to the random orientation of the unit

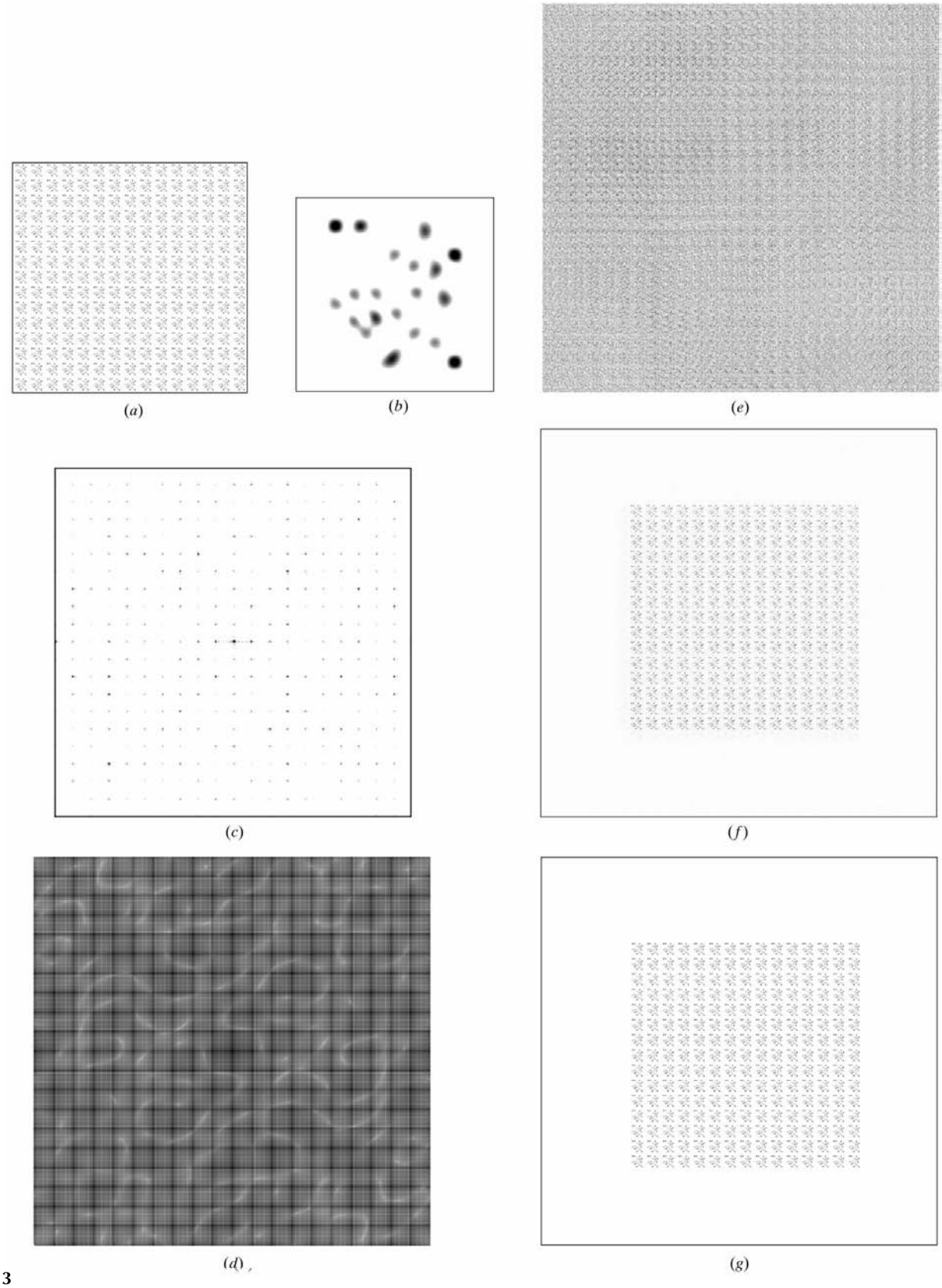

Figure 3
Phase retrieval of the oversampled diffraction pattern from a small 2D crystal. (*a*) The density of a small crystal with 15 × 15 unit cells (a 300 × 300 pixel array). (*b*) The electron density of the unit cell with a size of 5 × 5 nm and 25 randomly distributed 'atoms'. (*c*) The calculated oversampled diffraction pattern (a 512 × 512 pixel array) of the small crystal in linear scale. (*d*) Same as (*c*) but on logarithmic scale. (*e*) A density combining the diffraction pattern of (*c*) and a random initial phase set. (*f*) and (*g*) The reconstructed density after 50 and 400 iterations, respectively, with a loose support of a 312 × 312 pixel array. (*h*) The reconstructed unit cell after 400 iterations. (*i*) The convergence of the reconstruction. (*j*) The reconstructed density of the small crystal with SNR = 10. (*k*) The reconstructed unit cell with SNR = 10.

cells, this pattern displays a ring structure. By using positivity constraints on the real part, a random initial phase set and the same loose support, our algorithm perfectly reconstructs the electron density after 2800 iterations as shown in Fig. 5(*c*). We then add noise of SNR = 20 on the oversampled diffraction pattern and also nicely reconstruct the electron density.

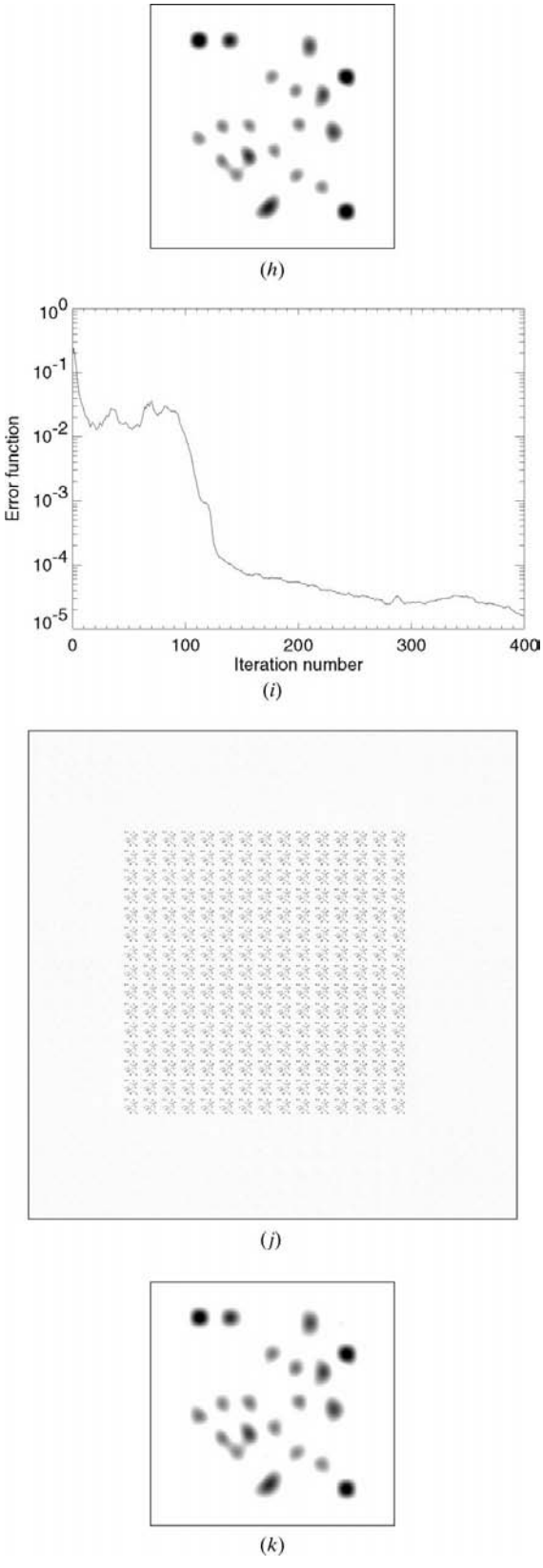

Figure 3 (continued)

The final example employs a single unrepeated motif. Fig. 6(*a*) shows the original density of a two-dimensional 'molecule' with a diameter of 75 nm and a total of 5625 atoms inside a 300 × 300 pixel array. We then calculate the oversampled diffraction pattern of the molecule shown in Fig. 6(*b*). By employing a random initial phase set, a loose support of a 78 × 78 nm (or 312 × 312 pixel) square with $\sigma = 2.7$ and positivity constraints on the real part, our algorithm reconstructs the density after 1800 iterations as shown in Fig. 6(*c*). We also succeed in reconstructing the density from a noisy diffraction pattern with SNR = 20. In the last three examples, we have also performed a few more reconstructions with different random initial phase sets and always succeed in recovering the phase, though the convergence speed is different in each case.

4. Radiation-damage problem

In §3, we showed that the oversampling technique is so powerful that it can retrieve the phase directly from the diffraction patterns of small crystals (either perfect or imperfect), repeated motif without orientational regularity, or single molecules. The crystallinity limitation of X-ray crystallography can thus be removed. Moreover, this technique is simple to employ and is generally successful without requiring any knowledge of the specimen's structure except for a loose support. The oversampling technique, however, has the disadvantage that it imposes a high radiation dose compared to the Bragg-point-only techniques. (At the Bragg points, the periodicity of the crystal produces, through constructive interference, a very large amplification of the intensity, of the order of the number of unit cells in the crystal.) This large coherency gain can greatly reduce the radiation damage to the specimens. With the oversampling technique, the intensity between Bragg peaks as well as the Bragg peaks for small crystals and the whole continuous and weak pattern for non-crystalline specimens have to be employed for phase retrieval. The coherency gain thus disappears and the specimens are subjected to a high radiation dose. A calculation by Sayre & Chapman (1995) showed that, in the case of X-ray diffraction of non-crystalline specimens, the dose rises approximately as the eighth power of the resolution. While material science specimens can withstand a high radiation dose, biological specimens are very sensitive to the dose. Gilbert & Pine (1992) demonstrated that a radiation dose of 10^5 Gray (1 Gray=100 rad) produces immediate morphological changes and structural deterioration in wet and living cells. X-ray microscopy studies have shown that, by using chemical fixation, wet biological specimens can stand up to 10^6 Gray radiation dose (Bennett *et al.*, 1993; Williams *et al.*, 1993) and dry biological specimens can be stable with radiation doses up to 10^7 Gray (Williams *et al.*, 1993).

To increase the radiation dose without affecting the observed structure of biological specimens, more advanced

techniques have to be employed. By cooling the specimens to liquid-nitrogen temperature, experiments (Maser *et al.*, 1998; Schneider & Niemann, 1998) have shown that the specimen can withstand a radiation dose up to 10^{10} Gray without observable morphological damage, which, according to Sayre and Chapman's result, corresponds to ~10 nm three-dimensional resolution. By combining the oversampling and the cryogenic technique, our previous work (Miao *et al.*, 1999*a*,*b*) should thus be extendable to image whole biological cells and large subcellular structures at ~10 nm resolution in three dimensions.

To achieve higher resolution, flash X-ray sources might be used to record the diffraction pattern. Theoretical studies by Solem & Baldwin (1982) and by London *et al.* (1989) concluded that, with exposure duration of a picosecond, biological specimens remain morphologically unchanged to an accuracy of 10 nm. With an even shorter pulse such as may be obtainable from free-electron lasers ($>10^{12}$ photons and <200 fs per pulse), better than 10 nm resolution may be achieved, though further studies of radiation damage to biological specimens by hard X-rays are needed. Free-electron lasers, however, cannot be used in a conventional tomographic scheme to reconstruct three-dimensional structures from a single specimen because the specimen will be completely destroyed after a powerful single pulse. To get a three-dimensional structure, multiple accurate copies of a specimen are thus needed. Fortunately, some very important biological specimens such as single protein or virus molecules can provide such copies. By combining the oversampling technique and free-electron lasers, we might therefore obtain high-resolution three-dimensional structure information of single protein or virus molecules. Apart from the alleviation of the radiation-damage problem, free-electron lasers also have other advantages over other X-ray sources such as synchrotron radiation. First, the combination of the oversampling technique and free-electron lasers can provide the structure

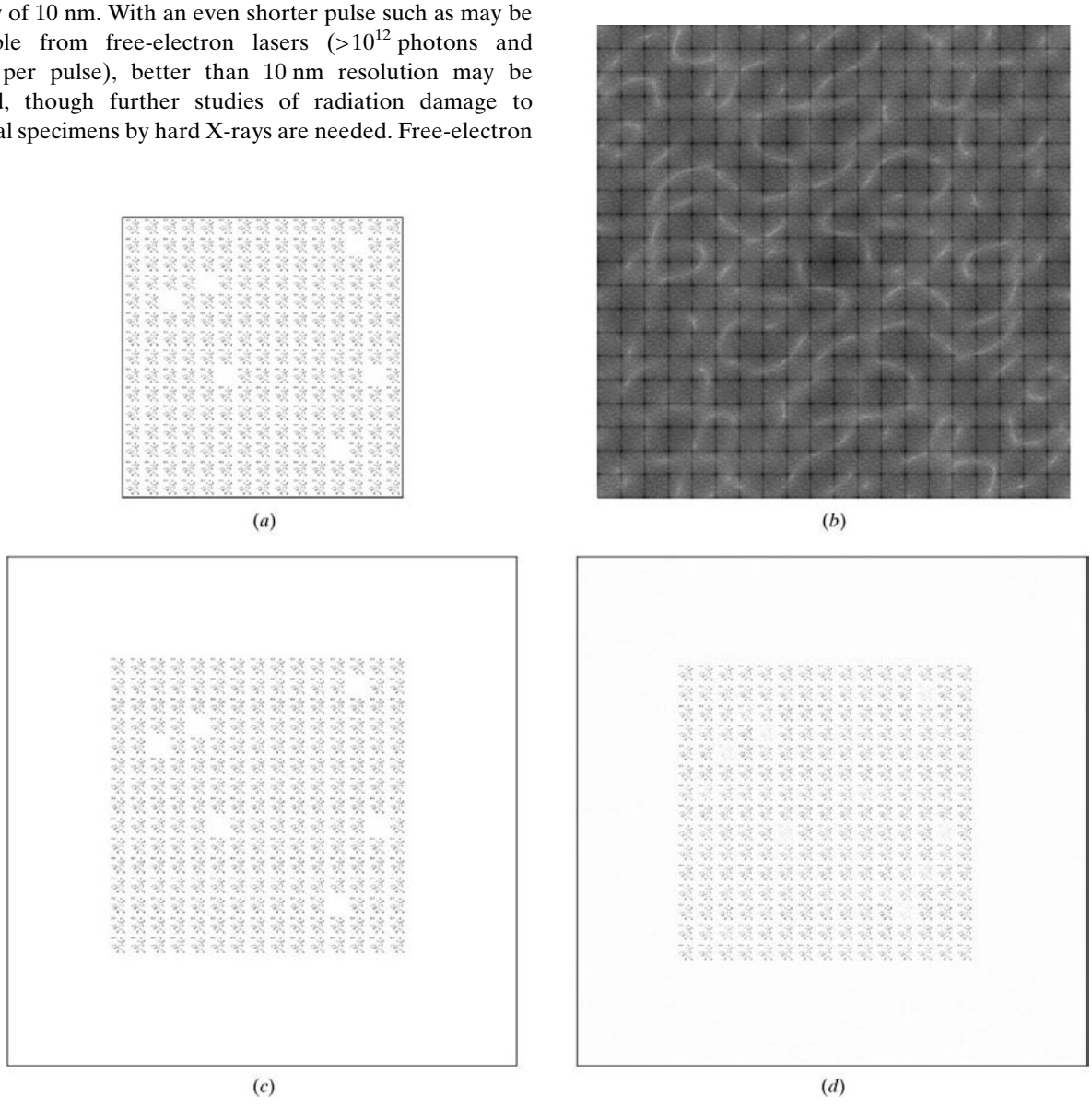

Figure 4
Phase retrieval of the oversampled diffraction pattern from a small crystal with six defects. (*a*) The density of a small crystal with six defects. (*b*) A calculated oversampled diffraction pattern (on logarithmic scale) from (*a*). (*c*) The reconstructed density after 1500 iterations with a random initial phase set and a loose support of $\sigma = 2.7$. (*d*) The reconstructed density with SNR = 20 after 2500 iterations.

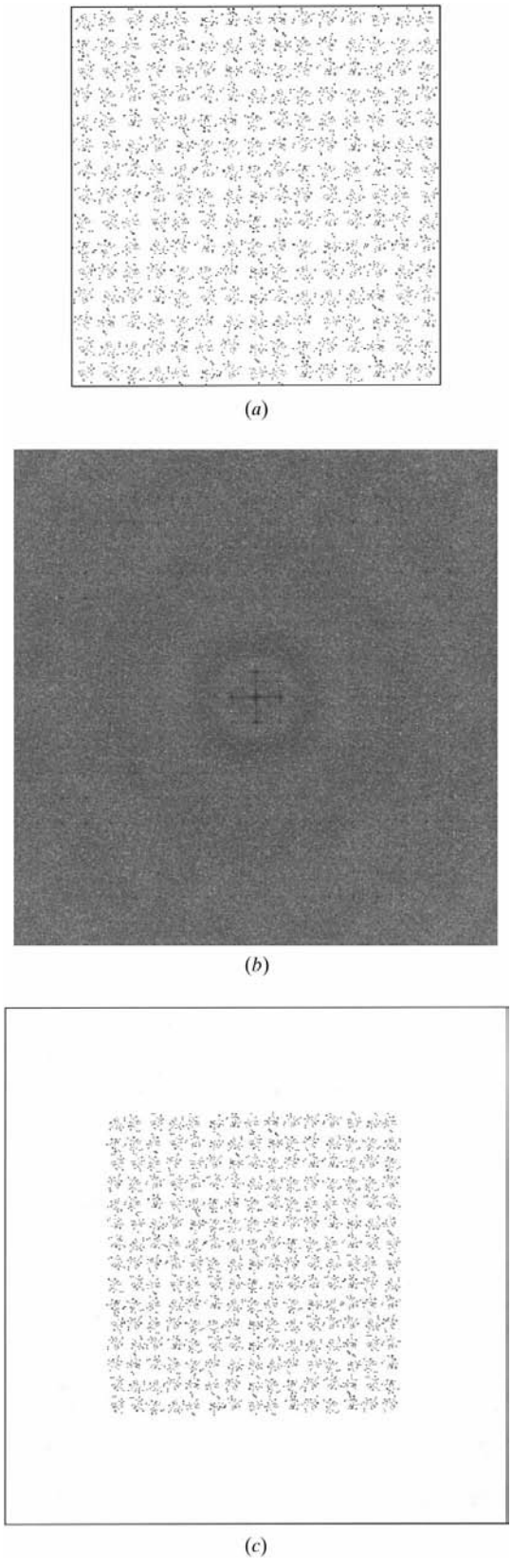

Figure 5
Phase retrieval of the oversampled diffraction pattern from a periodically translated and randomly oriented specimen. (*a*) The density of the specimen. (*b*) A calculated oversampled diffraction (on logarithmic scale) from (*a*). (*c*) The reconstructed density after 2800 iterations with a random initial phase set and a loose support of $\sigma = 2.7$.

determination not only of high spatial resolution but also of time resolution at the sub-picosecond level. Second, the oversampling technique has to record the weak intensity for phase retrieval where thermal motion of the atoms inside the specimen may disturb the high-resolution diffraction pattern. With free-electron lasers, the thermal-motion problem is a problem no more, since only a very fast snapshot of the specimen structure is caught in a diffraction pattern.

5. Conclusions

It is shown, in computer experiments, that the phase problem can be generally overcome in finite specimens (*viz* in small perfect or imperfect crystals; repeated motifs without orientational regularity; and unrepeated motifs, such as amorphous glasses, single molecules or single biological cells) by spatially finer measurement of diffraction-pattern intensity than has been customary in crystallography; *i.e.* by sampling at spatial finenesses in diffraction space corresponding to specimen (rather than unit-cell) dimensions. The technique requires no *ab initio* information beyond approximate knowledge of the specimen envelope, and appears to have a fair degree of robustness against noise in the intensity data. It requires, however, the measurement of many weak diffraction intensities and accordingly involves high radiation dosage to the specimen; it thus shifts the crystallinity and phasing problems of X-ray crystallography to the radiation-damage problem. The problem can be somewhat reduced by using cryogenic techniques and it may become possible to image biological specimens such as whole cells and large subcellular structures at ~10 nm resolution in three dimensions. In the long run, by employing free-electron lasers, it may be possible to circumvent the radiation-damage problem and allow the oversampling technique to open a new field for imaging biological specimens such as single protein or virus molecules at both high spatial resolution and sub-picosecond time resolution.

A main thrust of this paper is to go beyond Miao *et al.* (1999*a*) in pointing out that the imaging of (*a*) crystalline and (*b*) near-crystalline specimens, as well as of (*c*) non-crystalline specimens as treated in that paper, can be assisted by oversampling methods; in other words, to point out that oversampling may be able to assist within crystallography, as well as in extensions of crystallography. Specifically, this paper emphasizes that there are not one, but three, types of samplings that may be of interest in crystal structure analysis itself. The classical one of course is Bragg sampling, which provides the ultimate in low-dose/high-resolution imaging but which also faces the phase problem. The remaining two, through oversampling, are in principle freed from the phase problem. In one of these, the sampling is somewhat finer than Bragg sampling (see footnote at the end of §2), and thus must deal with higher, but perhaps not extremely higher, dose levels. In the third, the sampling is the finer-than-Nyquist sampling; the dosage level that must be dealt with is then very high indeed but the method is so general that the imaging can

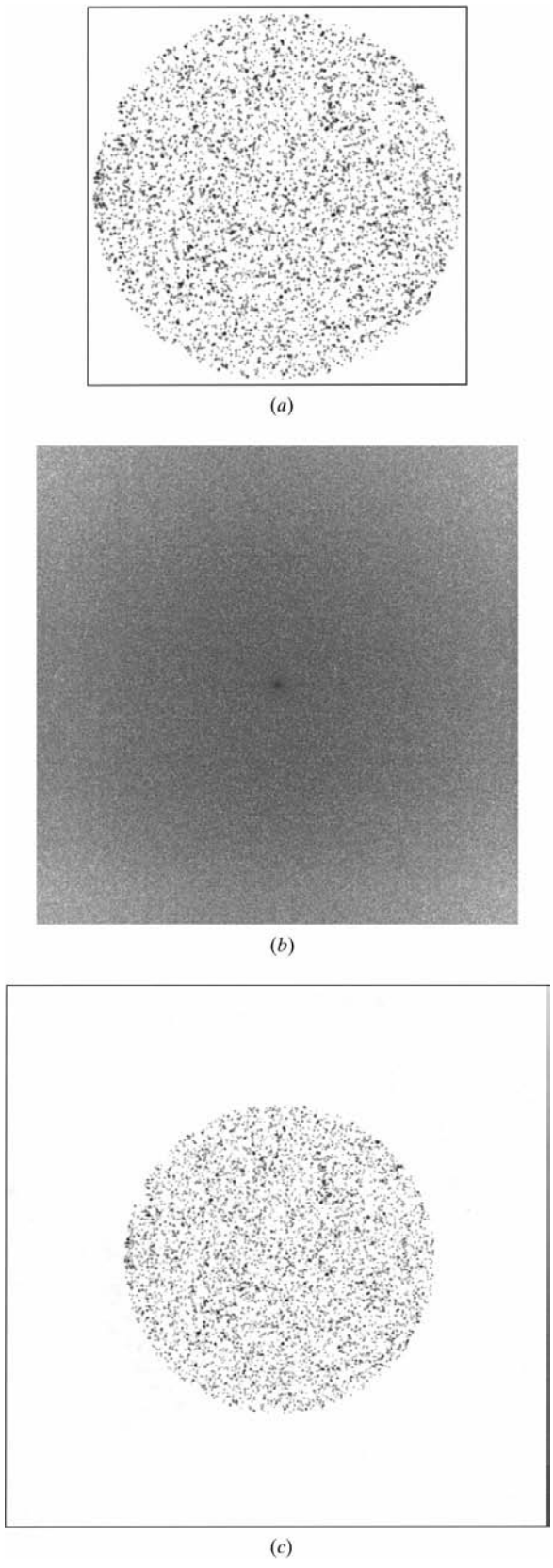

Figure 6
Phase retrieval of the oversampled diffraction pattern from a single unrepeated motif (molecule, amorphous glass, biocell *etc.*). (*a*) The density of the 'molecule'. (*b*) A calculated oversampled diffraction (on logarithmic scale) from (*a*). (*c*) The reconstructed density after 1800 iterations with a random initial phase set and a loose support of $\sigma = 2.7$.

extend to arbitrary defect variations on crystallinity (see Figs. 4 and 5).

APPENDIX *A*
Oversampling theorem

For convenience and brevity, we are here replacing the usual argument, which is through the convolution theorem and the reciprocal properties of lattices, by a short direct proof. If the density of an object is assumed to be $\rho(\mathbf{x})$, its Fourier transform is

$$F(\mathbf{k}) = \int_{-\infty}^{\infty} \rho(\mathbf{x}) \exp(2\pi i \mathbf{k} \cdot \mathbf{x})\, \mathrm{d}\mathbf{x}, \tag{7}$$

where $\mathbf{x}$ is the three-dimensional spatial coordinate in real space and $\mathbf{k}$ the three-dimensional frequency coordinate in reciprocal space. If we sample $F(\mathbf{k})$ at Nyquist frequency, we get

$$F(\mathbf{k}) = \sum_{\mathbf{x}=0}^{N-1} \rho(\mathbf{x}) \exp(2\pi i \mathbf{k} \cdot \mathbf{x}/N), \quad \mathbf{k} = 0, \ldots, N-1, \tag{8}$$

where $\mathbf{x}$ and $\mathbf{k}$ are discretized and range from 0 to $N-1$ in each dimension. If we sample $F(\mathbf{k})$ at twice the Nyquist frequency, we have

$$F(\mathbf{k}) = \sum_{\mathbf{x}=0}^{N-1} \rho(\mathbf{x}) \exp[2\pi i \mathbf{k} \cdot \mathbf{x}/(2N)], \quad \mathbf{k} = 0, \ldots, 2N-1. \tag{9}$$

We then introduce a new function

$$g(\mathbf{x}) = \begin{cases} \rho(\mathbf{x}) & 0 \leq \mathbf{x} \leq N-1 \\ 0 & N \leq \mathbf{x} \leq 2N-1. \end{cases} \tag{10}$$

By substituting (10) into (9), we have

$$F(\mathbf{k}) = \sum_{\mathbf{x}=0}^{2N-1} g(\mathbf{x}) \exp[2\pi i \mathbf{k} \cdot \mathbf{x}/(2N)], \quad \mathbf{k} = 0, \ldots, 2N-1. \tag{11}$$

Equation (11) represents the relation between a density function of $g(\mathbf{x})$ and its fast-Fourier-transform pattern sampled at Nyquist frequency. This process shows that oversampling the Fourier transform more densely than the Nyquist frequency generates a no-density region surrounding the electron density of the specimen.

The decision to try oversampling as a phasing technique was arrived at in a conversation between DS and G. Bricogne in the late 1980's. Dr G. Bonfiglioli, working independently in Italy, has recently been arriving at concepts similar to our own (private communications). The authors gratefully acknowledge Professor Janos Kirz, Physics Department, State University of New York at Stony Brook, for his invaluable contribution to the paper, and Professor Chris Jacobsen, of the same department, for the use of his computer facility. This work was supported by the US Department of Energy under grant DE-FG02-89ER60858.

References

Bates, R. H. T. (1982). *Optik (Stuttgart)*, **61**, 247–262.
Bennett, P. M., Foster, G. F., Buckley, C. J. & Burge, R. E. (1993). *J. Microsc.* **172**, 109–119.
Boyes-Watson, J., Davidson, K. & Perutz, M. F. (1947). *Proc. R. Soc. London Ser. A*, **191**, 83–132.
Bruck, Yu. M. & Sodin, L. G. (1979). *Optic. Commun.* **30**, 304–308.
Fienup, J. R. (1982). *Appl. Opt.* **21**, 2758–2769.
Gerchberg, R. W. & Saxton, W. O. (1972). *Optik (Stuttgart)*, **35**, 237–246.
Gilbert, J. R. & Pine, J. (1992). *Soft X-ray Microscopy. Proc. SPIE*, No. 1741, edited by C. Jacobsen & J. Trebes, pp. 402–408.
Henke, B. L., Gullikson, E. M. & Davis, J. C. (1993). *At. Data Nucl. Data Tables*, **54**, 181–342.
London, R. A., Rosen, M. D. & Trebes, J. E. (1989). *Appl. Opt.* **28**, 3397–3404.
Maser, J., Jacobsen, C., Kirz, J., Osanna, A., Spector, S., Wang, S. & Warnking, J. (1998). *X-ray Microscopy and Spectromicroscopy*, edited by J. Thieme, G. Schmahl, D. Rudolph & E. Umbach, pp. 35–44. Berlin: Springer-Verlag.
Miao, J., Chapman, H. N. & Sayre, D. (1997). *Microsc. Microanal.* **3** (Suppl. 2), 1155–1156.
Miao, J., Charalambous, C., Kirz, J. & Sayre, D. (1999*a*) *Nature (London)*, **400**, 342–344.
Miao, J., Charalambous, C., Kirz, J. & Sayre, D. (1999*b*). *X-ray Microscopy. Proceedings of the Sixth International Conference*, edited by W. Meyer-Ilse, T. Warwick & D. Attwood, pp. 581–586. New York: American Institute of Physics.
Miao, J., Sayre, D. & Chapman, H. N. (1998). *J. Opt. Soc. Am.* A**15**, 1662–1669.
Millane, R. P. (1990). *J. Opt. Soc. Am.* A**7**, 394–411.
Millane, R. P. (1993). *J. Opt. Soc. Am.* A**10**, 1037–1045.
Millane, R. P. (1996). *J. Opt. Soc. Am.* A**13**, 725–734.
Millane, R. P. & Stroud, W. J. (1997). *J. Opt. Soc. Am.* A**14**, 568–579.
Sayre, D. (1952). *Acta Cryst.* **5**, 843.
Sayre, D. (1991). *Direct Methods of Solving Crystal Structures*, edited by H. Schenk, pp. 353–356. *NATO ASI Ser. Ser. B (Physics)*, Vol. 274. New York: Plenum.
Sayre, D. & Chapman, H. N. (1995). *Acta Cryst.* A**51**, 237–252.
Sayre, D., Chapman, H. N. & Miao, J. (1998). *Acta Cryst.* A**54**, 232–239.
Schneider, G. & Niemann, B. (1998). *X-ray Microscopy and Spectromicroscopy*, edited by J. Thieme, G. Schmahl, D. Rudolph & E. Umbach, pp. 25–34. Berlin: Springer-Verlag.
Solem, J. C. & Baldwin, G. C. (1982). *Science*, **218**, 229–235.
Williams, S., Zhang, X., Jacobsen, C., Kirz, J., Lindaas, S., Van't Hof, J. & Lamm, S. S. (1993). *J. Microsc.* **170**, 155–165.
Woolfson, M. M. (1987). *Acta Cryst.* A**43**, 593–612.